

# Measurement compatibility in multiparameter quantum interferometry

Jayanth Jayakumar,<sup>1,2</sup> Marco Barbieri,<sup>3</sup> and Magdalena Stobińska<sup>2</sup>

<sup>1</sup>*Faculty of Physics, University of Warsaw, ul. Pasteura 5, 02-093 Warsaw, Poland*

<sup>2</sup>*Faculty of Mathematics, Informatics and Mechanics,  
University of Warsaw, ul. Banacha 2, 02-097 Warsaw, Poland*

<sup>3</sup>*Dipartimento di Scienze, Università degli Studi Roma Tre,  
Via della Vasca Navale 84, 00146 Rome, Italy*

(Dated: April 28, 2025)

While the performance of single-parameter quantum sensors is immediate to assess by means of the Cramér-Rao bound, extension to multiple parameters demands more caution. Different aspects need to be captured at once, including, critically, compatibility. In this article we consider compatibility in quantum interferometry for an important class of probe states and for double homodyne measurement, standard benchmarks for these applications. We include the presence of loss and phase diffusion in the estimation of a phase. Our results illustrate how different weighting of the precision on individual parameters affects their compatibility, adding to the list of considerations for quantum multiparameter estimation.

## I. INTRODUCTION

Quantum sensing holds promising perspectives for the observation of fragile materials with a reduced footprint [1–4]. Optimising the state of the probes and their measurement down to their quantum properties, strategies capable of enhanced precision can be conceived [5–11]. The actual implementation may then be confronted with further constraints, such as the availability of components, or trade-offs in their performance. The presence of undesired effects is almost always unavoidable, and these need to be considered in any realistic sensor [12–19]. Embracing a multiparameter setting, in which target and nuisance parameters are estimated at once, has been proposed as a way of making the estimation more robust [20–25].

This advantage, however, comes at the cost of apportioning the available information content of the probes among the different parameters [26, 27]. In fact, optimal measurements pertaining to individual parameters may not commute, preventing their joint optimal estimation. Therefore, *compatibility* becomes an outstanding aspect in the multiparameter scenario [28]. A possible way to capture it demands comparing two information metrics: on the one side, the quantum Fisher information matrix [29–31], on the other, Holevo information [32, 33]. The former quantifies the achievable variances assuming optimal measurement for each parameter. The latter, instead, develops on more sophisticated tools and delivers a bound on the variance that can be attained in principle, by a collective measurement on a large number of probes [34–39]. The bound from the Fisher information, known as the quantum Cramér-Rao bound (QCRB)  $C_Q$  [40–42], then assumes more relaxed conditions which may never be met in the experiment, hence the Holevo Cramér-Rao bound

(HCRB)  $C_H$  is considered the most relevant scalar bound in this scenario [43]. Since  $C_H$  is at most  $2C_Q$  [44–46], the quantity  $C_H/C_Q$ , introduced by Bellardo and Giovannetti, can be taken as an indicator quantifying the intrinsic compatibility of the problem [47].

The HCRB is established taking the most powerful possible measurements [48–52], but there exist instances in which simpler strategies are sufficient to closely saturate it [23, 34]. However, these are rather exceptional cases, and the typical situation in the typical times is that feasible measurements, foremost non-collective ones, are far from its saturation [53, 54], hence the importance of finding relevant figures of merit. In this article we draw inspiration from the Bellardo-Giovannetti ratio to devise a quantity that captures compatibility in a quantum interferometer. Our findings illustrate how attributing different weights to the different parameters translates to their compatibility when phase is estimated together with loss or phase diffusion. Our findings provide guidelines for inspecting the important issue of compatibility in practical cases.

## II. RESULTS

### A. The setting

We consider a Mach-Zehnder interferometer (MZI) as the model for quantum interferometry. The task then consists in estimating the relative phase between its two arms. However, for a comprehensive analysis, we should also include the presence of loss in both arms of the MZI, as well as some dephasing accounting for random fluctuations of the phase at faster time scales than the detection. These represent the main source of nuisance in realistic quantum

interferometric sensors.

It is often the case that the values of the noise parameters are unknown at the time of measurement, hence they must be estimated along with the phase. Therefore, our measurements should be sensitive to noise parameters as well: this is particularly relevant for those ranges in which phase sensitivity is affected the most. This strategy is known to make the estimation more reliable [55, 56], however, the maximal sensitivity on each parameter is affected by their reciprocal interplay. This is a typical instance even in classical multiparameter estimation, made more ravelled by the intricacies of quantum measurements. These aspects are quantitatively captured by the HCRB,  $C_H$ , against which the actual sensitivity of a specific measurement scheme should be benchmarked. The key aspect is then understanding how its attainability is hampered by the actual performance of the measurement. This can be understood as the result of correlations of the parameters in the outcome probabilities, that are different than those predicated at the quantum limit.

We consider as the input, probe states in the form of the generalized Holland-Burnett (gHB) and the Holland-Burnett (HB) states, which are a class of experimentally relevant two-mode fixed photon number states. Given the distinct physical origin of the types of noise, we analyze the sensitivities of measurements considering the joint estimation of phase with each noise parameter separately. The gHB states are created by the action of a balanced beam splitter on a two-mode Fock state  $|n, N-n\rangle$ , namely

$$|\Psi_{\text{gHB}}(n, N-n)\rangle = \mathcal{U}_{\text{BS}} |n, N-n\rangle \quad (1)$$

$$= \sum_{p=0}^N \mathcal{A}_N(n, p) |p, N-p\rangle \quad (2)$$

where  $\mathcal{U}_{\text{BS}} = \exp[-i\frac{\pi}{4}(a'^{\dagger}b' + b'^{\dagger}a')]$  is the beam splitter unitary operator;  $a', b'$  and  $a'^{\dagger}, b'^{\dagger}$  are the annihilation and creation operators, respectively, corresponding to the input modes of the beam splitter; and

$\mathcal{A}_N(n, p) = (-1)^n \sqrt{2^{-N} \binom{N}{n} \binom{N}{p}} {}_2F_1(-n, -p; -N; 2)$  are the Kravchuk coefficients [57]. The HB state is obtained as a special case of the gHB state at  $n = N/2$  i.e., when we interfere equal numbers of photons on a balanced beam splitter.

In the MZI, the input gHB state goes through a phase-shift operation in which photons in one arm acquire a relative phase  $\phi'$  with respect to the other. This is followed by an operation that introduces loss of photons in both arms modeled by beam splitters of transmissivities  $\eta_a$  and  $\eta_b$ . Furthermore, the phase diffusion operation is introduced by allowing the val-

ues of the acquired phase to vary randomly according to a Gaussian probability distribution  $p_{\phi, \Delta}(\phi')$  of mean  $\phi$  and standard deviation  $\Delta$ . In other words, we take a weighted average of the lossy state over all phase values with respect to  $p_{\phi, \Delta}(\phi')$ . All of these operations can be condensed into the equation

$$\rho_{\phi, \eta_a, \eta_b, \Delta}^{\text{gHB}}(n, N-n) = \int_{-\infty}^{\infty} p_{\phi, \Delta}(\phi') \left( \sum_{k=0}^N \sum_{l=0}^{N-k} K_{b, l, \eta_b} K_{a, k, \eta_a} \mathcal{U}_{\phi'} \rho^{\text{gHB}} \mathcal{U}_{\phi'}^{\dagger} K_{a, k, \eta_a}^{\dagger} K_{b, l, \eta_b}^{\dagger} \right) d\phi', \quad (3)$$

where  $\mathcal{U}_{\phi'} = e^{-i\hat{a}^{\dagger} \hat{a} \phi'}$  is the phase-shift operation and  $\hat{a}$  is one of the output modes of the beamsplitter. If  $k$  and  $l$  photons are lost from the modes  $a$  and  $b$ , respectively, then  $K_{a, k, \eta_a} = \sqrt{\frac{(1-\eta_a)^k}{k!}} \sqrt{\eta_a^{\hat{a}^{\dagger} \hat{a}}} \hat{a}^k$ ,  $K_{b, l, \eta_b} = \sqrt{\frac{(1-\eta_b)^l}{l!}} \sqrt{\eta_b^{\hat{b}^{\dagger} \hat{b}}} \hat{b}^l$  are the Kraus operators that make up the photon loss channel, and  $p_{\phi, \Delta}(\phi') = \frac{1}{\sqrt{2\pi\Delta^2}} e^{-(\phi' - \phi)^2 / 2\Delta^2}$

After evaluating the operations in Eq. 3, we obtain

$$\begin{aligned} & \rho_{\phi, \eta_a, \eta_b, \Delta}^{\text{gHB}}(n, N-n) \\ &= \sum_{k=0}^N \sum_{l=0}^{N-k} \sum_{p, q=k}^{N-l} \mathcal{C}_{\phi, \eta_a, \eta_b, \Delta}^N(n, p, q) \\ & \quad \times |p-k, N-p-l\rangle \langle q-k, N-q-l|, \end{aligned} \quad (4)$$

where  $\mathcal{C}_{\phi, \eta_a, \eta_b, \Delta}^N(n, p, q) = \mathcal{A}_N(n, p) \mathcal{A}_N(n, q) e^{-i(p-q)\phi - \frac{\Delta^2}{2}(p-q)^2} \sqrt{B_{kl}^p B_{kl}^q}$ ,  $B_{kl}^p = \binom{p}{k} \binom{N-p}{l} \eta_a^{p-k} (1-\eta_a)^k \eta_b^{N-p-l} (1-\eta_b)^l$  quantifies the modification of the probability amplitudes due to losses.

Fixed-photon number states are generally associated with a measurement of the photon number at the two outputs of the MZI. This option typically shows good performance in quantum phase estimation, however it requires detectors in cryogenic environments, which may not be suitable for all applications. In this work, we focus instead on the use of a homodyne detector on each arm. While this explicitly demands a phase reference, this requirement has fewer technical constraints, and offers *per se* higher efficiencies.

In a general framework, we consider the estimation of  $p$  parameters, represented as a vector  $\vec{\theta} = (\theta_1, \dots, \theta_p)$  belonging to the parameter space  $\Theta \subset \mathbb{R}^p$ . The gHB state  $|\Psi_{\text{gHB}}\rangle$  has dimension  $d$  and lives in the Hilbert space  $\mathcal{H} \equiv \mathbb{C}^d$ . The corresponding density matrix (input probe state)  $\rho_{\text{gHB}}$  belongs to the space of  $d \times d$  Hermitian operators,

$\mathcal{L}(\mathcal{H}) \equiv \mathbb{C}^{d \times d}$ . Information about the parameters can be extracted using a suitable measurement  $M$  characterized by the positive operator-valued measure (POVM)  $\{\Pi_x\}$ . Thus, the action of  $M$  with respect to the output probe state  $\rho_\theta^{\text{gHB}}$  gives rise to a probability distribution  $\text{Tr}(\rho_\theta^{\text{gHB}} M) = p_\theta(x)$ . Classically, it is desirable for  $p_\theta(x)$  to be sensitive to small changes in the parameter values, and, consequently, this aspect is key to establish a metric to the performance of the measurement on the state. Considering  $\nu$  separable copies of the probe, which introduces another classical advantage, the performance of the measurement can be related to the precision of estimating the parameters through the Cramér-Rao bound (CRB) reading

$$\text{Tr}(W\Sigma) \geq \frac{1}{\nu} \text{Tr}(W F_C^{-1}) = C_C(M, \rho_\theta^{\text{gHB} \otimes \nu}, W, \vec{\theta}) \quad (5)$$

where  $\text{Tr}(W\Sigma)$  is the average cost,  $\Sigma_{i,j} = \int p_\theta(x) (\tilde{\theta}_i - \theta_i)(\tilde{\theta}_j - \theta_j) dx$  is the covariance matrix of unbiased estimators  $\tilde{\theta}_i$  with  $\Sigma_{i,i}$  representing the estimation precision for each parameter.  $F_C$  is the Fisher information matrix (FIM) whose elements read  $F_{C,i,j} = \int \frac{1}{p_\theta(x)} \left( \frac{\partial p_\theta(x)}{\partial \theta_i} \right) \left( \frac{\partial p_\theta(x)}{\partial \theta_j} \right) dx$ . In particular,  $F_{C,i,i}$  is the Fisher information (FI) that can be associated to each parameter when the others are known to arbitrary precision. Finally,  $W$  is a non-negative definite weight matrix belonging to the space of  $p \times p$  real matrices  $\mathcal{S}^{\mathbb{R}}(\Theta) \subset \mathbb{R}^{p \times p}$ , providing a penalty for the inaccurate estimation for each parameter. When  $\theta_i$  are the parameters of interest, then  $W$  is diagonal.

The quantum aspect of estimation theory is now introduced in order to obtain a measurement-independent quantum Cramér-Rao bound (QCRB) which depends only on the probe state:

$$\text{Tr}(W\Sigma) \geq \frac{1}{\nu} \text{Tr}(W F_Q^{-1}) = C_Q(\rho_\theta^{\text{gHB} \otimes \nu}, W, \vec{\theta}) \quad (6)$$

where  $F_Q$  is the quantum Fisher information matrix (QFIM) whose elements read  $F_{Q,i,j} = \text{Re}(\text{Tr}(\rho_\theta^{\text{gHB} \otimes \nu} L_{\theta_i} L_{\theta_j})) = \frac{1}{2} \text{Tr}(\rho_\theta^{\text{gHB} \otimes \nu} \{L_{\theta_i}, L_{\theta_j}\})$ ,  $L_{\theta_i}$  is the symmetric logarithmic derivative (SLD) for the parameter  $\theta_i$ . In particular  $F_{Q,i,i}$  is the quantum Fisher information (QFI) for each parameter. The QFI represents the amount of information about a parameter contained in the probe state. However, the QCRB does not provide a recipe for the optimal measurement, nor does it ensure it actually exists. The reason is that the optimal measurements associated with distinct parameters may not commute; hence, their joint estimation at the ultimate quantum precision may not be attained.

A more nuanced simultaneous optimization of estimators and the measurements gives rise to a bound that is stronger and tighter than the QCRB known as the HCRB as follows.

$$\text{Tr}(W\Sigma) \geq C_H(\rho_\theta^{\text{gHB} \otimes \nu}, W, \vec{\theta}) \quad (7)$$

The bound  $C_H$  is obtained as the outcome of the following convex optimization problem:

$$C_H(\rho_\theta^{\text{gHB} \otimes \nu}, W, \vec{\theta}) = \frac{1}{\nu} \min_{\vec{X}, V} \left[ \text{Tr}(WV) \mid V \geq Z(\vec{X}), \text{Tr}(\nabla \rho_\theta^{\text{gHB} \otimes \nu} \vec{X}^T) = \mathbf{1} \right] \quad (8)$$

where  $\vec{X} = (X_1, \dots, X_p)$  is a vector of  $p$  Hermitian matrices such that  $X_i \in \mathcal{L}(\mathcal{H})$ ,  $Z(\vec{X}) = \text{Tr}(\rho_\theta^{\text{gHB} \otimes \nu} \vec{X} \vec{X}^T)$  belongs to the space of  $p \times p$  complex matrices  $\mathcal{S}^{\mathbb{C}}(\Theta) \subset \mathbb{C}^{p \times p}$ ,  $V$  is a  $p \times p$  real matrix belonging to  $\mathcal{S}^{\mathbb{R}}(\Theta)$ , and  $\text{Tr}(\nabla \rho_\theta^{\text{gHB} \otimes \nu} \vec{X}^T) = \mathbf{1}$  is the local unbiasedness condition. The HCRB is known to be attainable under very general conditions, which, however, may have limited relevance in the practical case. More details are presented in [V A](#).

## B. Measurement compatibility measure

The two quantum bounds describe ultimate limits to the precision, with the HCRB being more pertinent in the practical case. This has led Belliardo and Giovannetti to introduce a figure of merit with the aim of quantifying compatibility as [\[47\]](#)

$$r_{BG}(\rho_\theta^{\text{gHB}}, W, \vec{\theta}) = \frac{C_H(\rho_\theta^{\text{gHB}}, W)}{C_Q(\rho_\theta^{\text{gHB}}, W)}. \quad (9)$$

This describes how close the best possible measurement scheme can get to the predicament of the QCRB, setting the intrinsic level of incompatibility in this estimation problem. In the analysis of practical cases, one is actually interested in understanding what extra cost is associated to the use of a specific measurement strategy, therefore a suitable figure is given by

$$r_H^C(M, \rho_\theta^{\text{gHB}}, W, \vec{\theta}) = \frac{C_C(M, \rho_\theta^{\text{gHB}}, W)}{C_H(\rho_\theta^{\text{gHB}}, W)} \quad (10)$$

This quantifies the compatibility offered by a chosen measurement  $M$ . Note that these measures are independent of  $\nu$  when separable probe states are considered, and for our analysis, we deal with a single

copy of the probe i.e.,  $\nu = 1$ , and hence we have denoted  $\rho_{\theta}^{\text{gHB} \otimes \nu}$  as  $\rho_{\theta}^{\text{gHB}}$  in Eqs. 9 and 10. Since  $C_C \geq C_H \geq C_Q$ , one can see that  $r_H^C \in [1, \infty)$ , with  $r_H^C = 1$  implying full measurement compatibility, where the measurement saturates the HCRB, while  $r_H^C \gg 1$  indicates low compatibility. This condition could be influenced by the relative weights associated to the parameters, thus the scope of prioritising and penalising the error on one parameter over the other is relevant. Towards this goal, we work with  $W(y) = \begin{bmatrix} 2y & 0 \\ 0 & 2(1-y) \end{bmatrix}$ ,  $y \in [0, 1]$ . By this choice, we can interpolate from the identity matrix, corresponding to  $y = 0.5$ , for an unbiased penalization, to the extremal cases  $y = 0$  and  $y = 1$ , yielding rank-1 matrices that penalize the error of only one of the two parameters. This also allows us to obtain bounds on linear combinations of estimation errors of individual parameters.

As for the evaluation of  $r_H^C$ ,  $C_C$  is evaluated numerically in a straightforward manner. However, to compute  $C_H$ , we note that Eq. 8 can be readily formulated as a semidefinite program (SDP), which can then be cast into a numerically solvable model [58]. We make use of the source code for the HCRB function from the `QuanEstimation` package [59], which feeds the numerical model to the `CVXPY` modeling framework in Python. For gHB states, particularly those of higher dimensions, we have further improved and optimized this code and solved the SDP using the `MOSEK` solver [60]. The code is available at [61]. For the evaluation of  $r_{BG}$ ,  $C_Q$  is computed numerically using the `QuanEstimation` package.

### C. Joint-estimation of phase and loss

#### 1. Phase and loss in one arm

The first application of the general setting described in Section II A concerns the joint estimation of phase and loss in one arm of the interferometer [21]. The corresponding output probe state  $\rho_{\phi, \eta_a}^{\text{gHB}}$  is obtained from Eq. 4 by setting  $\eta_b = 1$  (no loss on the reference arm),  $\Delta = 0$  (no dephasing). Crucially, this output has a direct sum structure  $\rho_{\phi, \eta_a}^{\text{gHB}}(n, N - n) = \bigoplus_{k=0}^N p_k |\xi_{\phi, \eta_a}(k)\rangle \langle \xi_{\phi, \eta_a}(k)|$ , where each term  $|\xi_{\phi, \eta_a}(k)\rangle = \frac{1}{\sqrt{p_k}} \sum_{p=k}^N \mathcal{A}_N(n, p) e^{-ip\phi} \sqrt{B_k^p} |p - k, N - p\rangle$  is a pure state belonging to the subspace corresponding to the loss of  $k$  photons, with a normalization factor  $p_k$  [15, 21]. These states also satisfy orthogonality  $\langle \xi_{\phi, \eta_a}(k), \xi_{\phi, \eta_a}(k') \rangle = \delta_{kk'}$ . Although we have computed the QCRB numerically here, the linearity of QFI on direct sums [29, 62] allows us, in principle,

to calculate the QCRB analytically.

Fig. 1 depicts the measurement compatibility measure  $r_H^C$  and the fundamental compatibility measure  $r_{BG}$  as a function of the weight  $y$  for our choice of double homodyne measurement on different probe states. The bounds depend on the value of the estimated parameter  $\eta_a$ , but are independent of  $\phi$ . Specifically, in panel (a), we consider HB states for  $N = 2, 4, 6, 8$ , in panel (b), we consider the gHB states:  $|\Psi_{\text{gHB}}(0, N)\rangle$  for  $N = 2, 3, 4, 5, 6, 7, 8$ . We compute the CRB, QCRB, and HCRB at  $\eta_a = 0.5$  so that the compatibilities are studied in scenario of moderate loss. Notice that the extreme points  $y = 0$  and  $y = 1$  correspond to a single-parameter estimation, thus the notion of compatibility does not apply.

In panel 1(a), for all values of  $N$ ,  $r_H^C$  shows a similar behaviour, with a minimum value achieved around  $y = 0.2$ , corresponding to the maximal compatibility allowed by our choice of measurement. As  $N$  increases, the overall magnitude of  $r_H^C$  also increases, signalling that double homodyne becomes more inefficient at extracting information. We can thus investigate whether this is at least partly mirrored in the behaviour of the fundamental compatibility  $r_{BG}$ . This reaches the value 1 at the extremes, as expected for single-parameter problems, and exhibits a maximum around  $y = 0.2$ , only weakly depending on  $N$ . On the other hand, fundamental incompatibility too increases with the number of photons, as  $r_H^C$  does, although on a different scale.

In panel 1(b), there occurs an increase of  $r_H^C$  as a function of  $N$ , but this dependency is much less pronounced. In contrast to panel (a), the best compatibility conditions for  $r_H^C$  occur in proximity of pure phase estimation, close to  $y = 0.9$ , corresponding to maximal measurement compatibility. Interestingly, we find that, at the level of individual photon number, the behavior of  $r_H^C$  mirrors that of  $r_{BG}$ . The latter also follows the behavior observed in panel (a). However at the collective level, in contrast to measurement compatibility, the fundamental compatibility remains constant with the number of photons.

#### 2. Phase and loss in both arms

In our second application, we study the joint estimation of phase and loss in one arm of the interferometer, while assuming a known amount of loss in the other arm. The corresponding output probe state  $\tilde{\rho}_{\phi, \eta_a}^{\text{gHB}}$  is obtained from Eq. 4 by setting  $\eta_b = 0.5$  (50% loss on the reference arm) and  $\Delta = 0$ . The output can be expressed as  $\tilde{\rho}_{\phi, \eta_a}^{\text{gHB}}(n, N - n) = \sum_{k=0}^N \sum_{l=0}^{N-k} p_{kl} |\xi_{\phi, \eta_a}(k, l)\rangle \langle \xi_{\phi, \eta_a}(k, l)|$ , where each term  $|\xi_{\phi, \eta_a}(k, l)\rangle =$

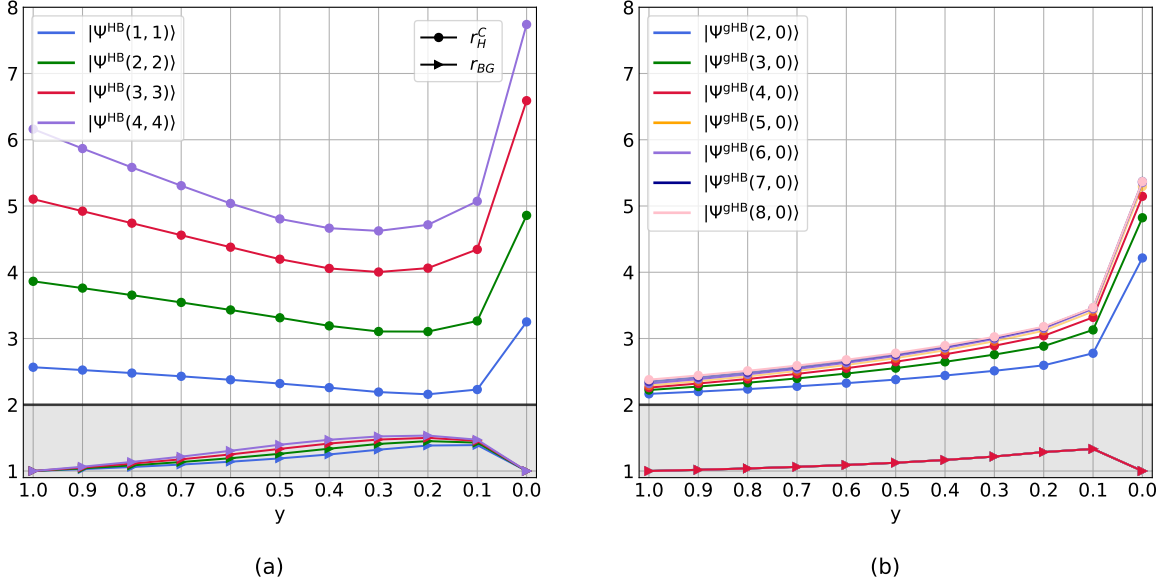


FIG. 1. Plot of measurement compatibility measure  $r_H^C$  and fundamental compatibility measure  $r_{BG}$  versus the weights  $y$  for the joint-estimation of phase and losses in one arm of the MZI. HB states with  $N = 2, 4, 6, 8$  (panel (a)) and gHB states with  $N = 2, 3, 4, 5, 6, 7, 8$  (panel (b)), and double homodyne measurement are considered. The curves are plotted at  $\eta_a = 0.5$  and  $\Delta = 0$ . Note that for HB states, the measurement compatibility decreases significantly as  $N$  increases, while the fundamental compatibility decreases only slightly as  $N$  increases.

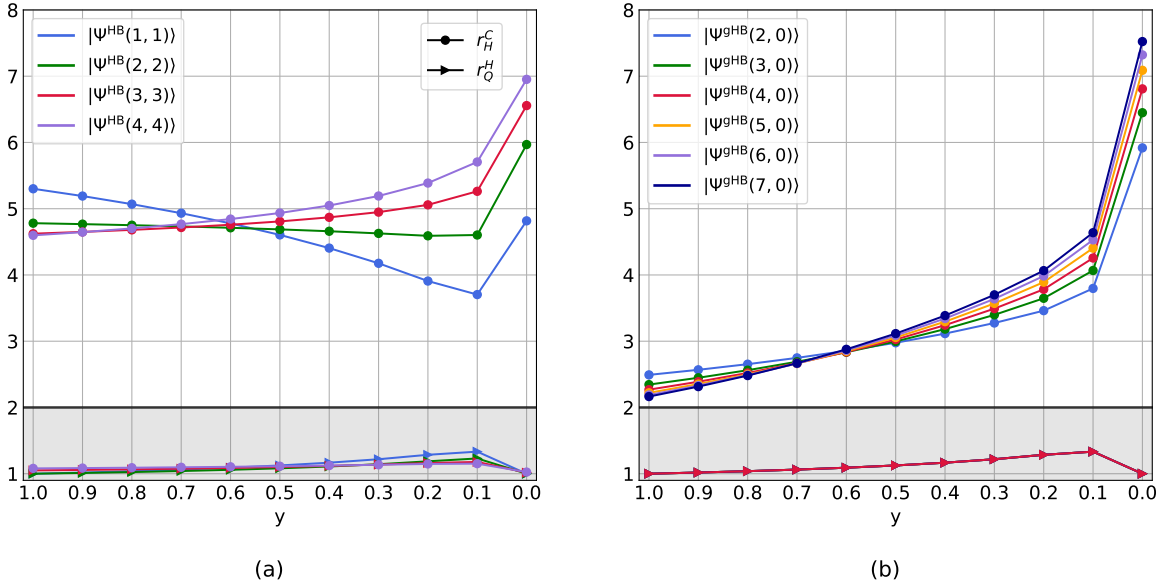


FIG. 2. Plot of measurement compatibility measure  $r_H^C$  and fundamental compatibility measure  $r_{BG}$  versus the weights  $y$  for the joint-estimation of phase and losses in one arm of the MZI with a known amount of loss on the reference arm. HB states with  $N = 2, 4, 6, 8$  (panel (a)) and gHB states with  $N = 2, 3, 4, 5, 6, 7$  (panel (b)), and double homodyne measurement are considered. The curves are plotted at  $\eta_a = 0.5$ ,  $\eta_b = 0.5$ , and  $\Delta = 0$ . Note that for HB and gHB states, the measurement compatibility exhibits an intersection at  $y = 0.6$ , causing its behavior with respect to  $N$  to change on either side of this point. In contrast, the fundamental compatibility increases slightly as  $N$  increases.



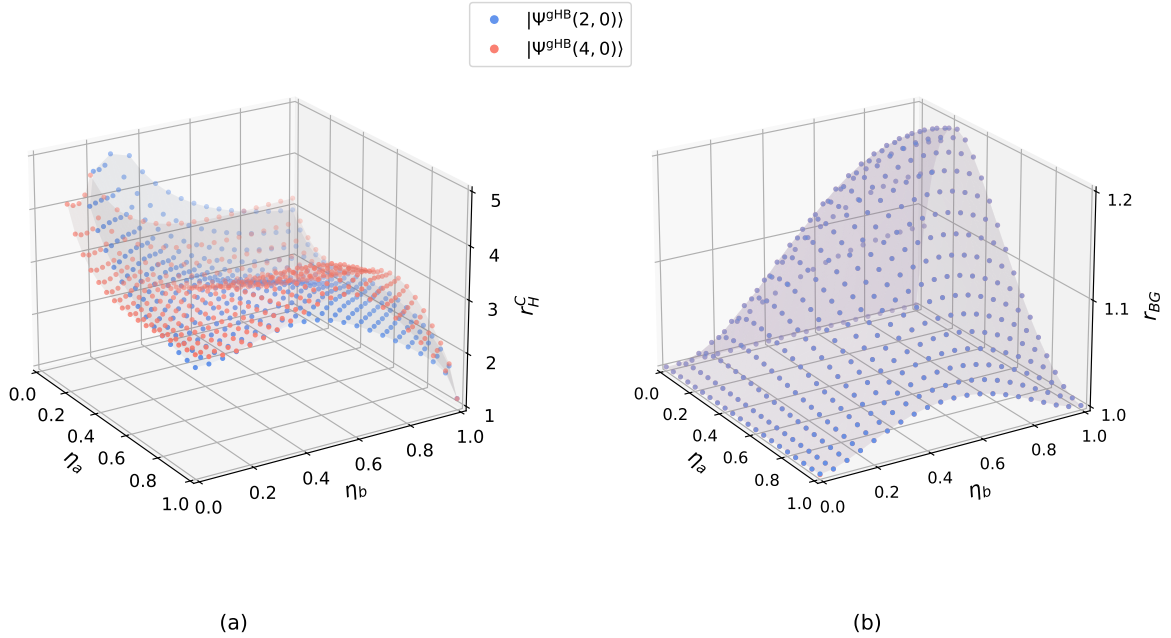


FIG. 3. *Joint-estimation of phase and loss*: Three-dimensional plots of measurement compatibility  $r_H^C$  (panel (a)) and fundamental compatibility  $r_{BG}$  (panel (b)) seen as a function of the losses,  $\eta_a$  and  $\eta_b$ , in each arm with equal parameter weights i.e., at  $y = 0.5$ . The probe state considered here is the gHB state  $|\Psi_{\text{gHB}}(0, N)\rangle$  with  $N = 2$  (blue dots) and  $N = 4$  (red dots) which create smooth surfaces. Note that the points closer to low values of losses exhibit high measurement and fundamental compatibilities. Also, the fundamental compatibility does not vary with respect to the chosen values of  $N$  for almost all pairs of values of losses.

$\frac{1}{\sqrt{p_{kl}}} \sum_{p=k}^{N-l} \mathcal{A}_N(n, p) e^{-ip\phi} \sqrt{B_{kl}^p} |p-k, N-p-l\rangle$  is a pure state conditioned on the number of lost photons,  $k$  and  $l$ , in each arm [15]. In general,  $\tilde{\rho}_{\phi, \eta_a}^{\text{gHB}}$  does not have a direct sum structure since the states corresponding to the same total number of lost photons  $m = k + l$  do not satisfy orthogonality. However, we note that, due to the convexity of QFI [29, 62], one can still obtain an analytical upper bound to the QFI but it is beyond the scope of this article.

In Fig. 2, we plot  $r_H^C$  and  $r_{BG}$  as a function of  $y$  for the double measurement on different probe states. Specifically, in panel (a), we consider HB states for  $N = 2, 4, 6, 8$ , in panel (b), we consider the gHB states:  $|\Psi_{\text{gHB}}(0, N)\rangle$  for  $N = 2, 3, 4, 5, 6, 7$ , and compute the CRB, QCRB, and HCRB at  $\eta_a = 0.5$ .

In panel 2(a), we observe different orderings in compatibility for phase and loss depending on the photon number  $N$ . When phase has more weight,  $y \simeq 1$ , increasing the photon number appears advantageous for  $r_H^C$ : one can attribute this to more distinct fringes in the probabilities of the two-homodyne outcomes. On the other hand, when loss has more weight,  $y \simeq 0$ , lower  $N$  results in better compatibility. As a consequence, the curves show an intersection around  $y = 0.6$ . The inspection of the fundamental incompatibility via  $r_{BG}$  reveals that this fea-

ture is specific to our choice of measurement, with higher  $N$  allowing for better compatibility, at a difference with respect to the previous case. In panel 2(b), the same trends are found for the double homodyne measurement, with an intersection occurring around  $y = 0.6$ . Both the individual and the collective behaviours of  $r_{BG}$  remain the same as in Fig. 1 (b). An investigation for generic loss reveals that the crossing point depend on the level of loss. Looking at the extreme cases, it is found that, for high losses on the reference arm ( $\eta_b = 0.1$ ),  $r_H^C$  decreases as  $N$  increases irrespectively on  $y$ , whereas for low losses ( $\eta_b = 1$ ), it increases with  $N$  for all values of  $y$  (see Section V B).

An analysis at different levels of losses  $\eta_a$  and  $\eta_b$  is reported in Fig. 3, illustrating the performance in terms of compatibility of different states for equal weights for the two parameters,  $y = 0.5$ . For moderate loss, compatibility only shows a weak dependence on  $\eta_a$  and  $\eta_b$ , while a decrease in transmission entails a decrease of compatibility as  $N$  grows. Inspection of the fundamental compatibility  $r_{BG}$  shows that, in the central region, compatibility is not assured for intermediate loss: this makes it relatively easier to approach the Holevo limit with a realistic measurement.

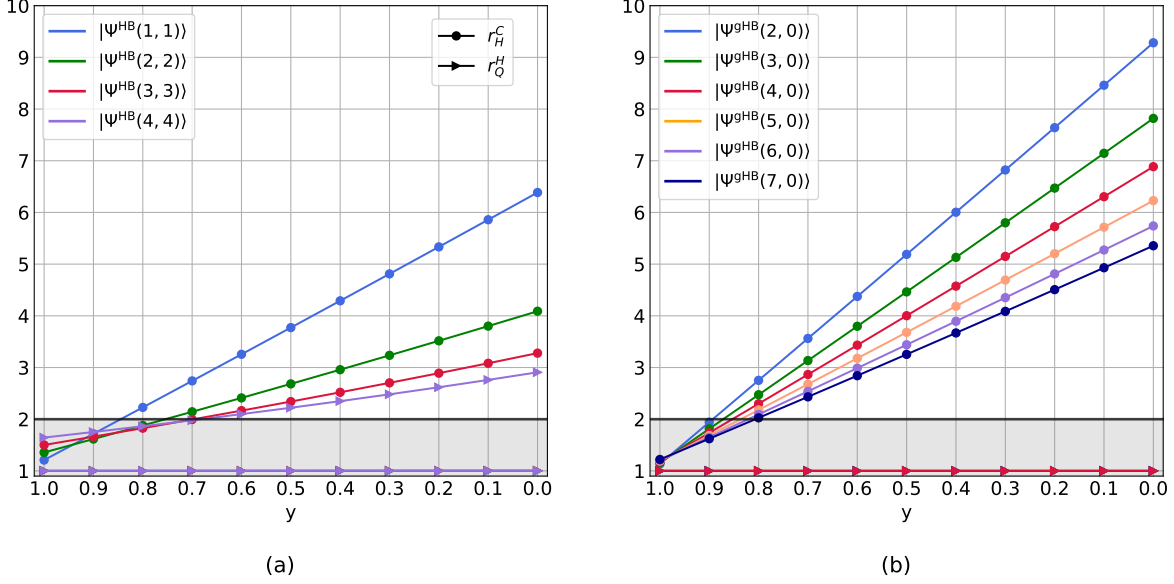


FIG. 4. Plot of measurement compatibility measure  $r_H^C$  and fundamental compatibility measure  $r_{BG}$  versus the weights  $y$  for the joint-estimation of phase and phase diffusion in the MZI with equal losses in both arms. HB states with  $N = 2, 4, 6, 8$  (panel (a)) and gHB states with  $N = 2, 3, 4, 5, 6, 7$  (panel (b)), and double homodyne measurement are considered. The curves are plotted at  $\eta = 0.999$  and  $\Delta = 0.1$ .

#### D. Joint-estimation of phase and phase diffusion

In last example, we consider the joint estimation of phase and phase diffusion while assuming known amount of losses in both arms. For simplicity, the output probe state  $\rho_{\phi,\Delta}^{\text{gHB}}$  is obtained from Eq. 4 by setting equal amount of losses in both arms,  $\eta_a = \eta_b = \eta$ , yielding  $\rho_{\phi,\Delta}^{\text{gHB}}(n, N-n) = \sum_{k=0}^N \sum_{l=0}^{N-k} \sum_{p,q=k}^{N-l} \mathcal{C}_{\phi,\Delta}^N(n, p, q) |p-k, N-p-l\rangle \langle q-k, N-q-l|$ .

In Fig. 4, panel (a) represents the plots of  $r_H^C$  and  $r_{BG}$  versus  $y$  for HB states with  $N = 2, 4, 6, 8$  and panel (b) represents the same plots for gHB states with  $N = 2, 3, 4, 5, 6, 7$ . We set  $\Delta = 0.1$  and  $\eta = 0.999$  (99.9% transmission loss in both arms).

Firstly, we report a recognisable behavior of  $r_{BG}$ : since phase and phase diffusion correspond to observables that are weakly compatible i.e.,  $\text{Tr}(\rho_{\phi,\Delta}^{\text{gHB}}[L_\phi, L_\Delta]) = 0$  [23–25], the system reaches maximal fundamental compatibility i.e.,  $r_{BG} = 1$  for all values of  $y$  in both panels. As for the behavior of  $r_H^C$ , in panel (a), we find an inversion of the ordering as for the case of loss in Fig. 2., but this time with the opposite trends. The curves intersect around  $y = 0.9$  due to which, for  $y \leq 0.9$ , the overall magnitude of  $r_H^C$  increases as  $N$  increases, whereas for  $y > 0.9$ , the magnitude decreases as  $N$  increases. In panel (b), most features observed in panel (a) re-

main the same, except that the dependence of  $r_H^C$  on  $N$  at  $y = 1$  is much less pronounced.

### III. DISCUSSION

The figure of merit for measurement compatibility,  $r_H^C$ , offers insight on attaining the HCRB with a chosen measurement strategy in a multiparameter setting. On analyzing the single parameter bounds for the estimation of phase and loss, we can remark on the following features. Our numerics show that, independently on  $N$ , the QFI for loss in HB and gHB probe states is always larger than that for phase. At the measurement level, however, this condition is not necessarily met by the FI matrix of the double homodyne measurement. If one considers the optimal states for phase and loss estimation, there is a crossing of the QFIs for loss and phase exactly at  $\eta = 0.5$ . As a result, one can infer that in the regime of high loss i.e.,  $\eta < 0.5$ , it is harder to estimate phase than loss, whereas in the regime of low loss i.e.,  $\eta > 0.5$ , it is harder to estimate loss than phase.

In Figs. 1-4, we have inspected the behavior of the two measures of compatibility under lossy scenarios. To further elucidate the connection between compatibility and losses in the system, we consider an ideal scenario of minimal losses i.e.,  $\eta_a = \eta_b = 0.999$ ,  $\Delta = 0$  in Eq. 4 while estimating phase and loss in one arm jointly. Considering HB and gHB states with

$N = 2, 4, 6$ , numerical results show that  $r_{BG} \approx 1$  for all values of  $y$ , indicating maximal fundamental compatibility. As for the measurement compatibility, we find that the  $r_H^C \approx 1$  at  $y = 1$  reaching maximal measurement compatibility due to the optimality of the double homodyne measurement in estimating phase [23]. Remarkably,  $r_H^C$  remains below 1.5 for  $y \geq 0.5$  for all the probe states considered (see Section V C), hence the double homodyne measurement closely attains the HCRB even with individual copies. This can be understood by considering that  $r_H^C$  can be approximated as

$$r_H^C = \frac{2y(F_{C\phi})^{-1} + 2(1-y)(F_{C\eta})^{-1}}{2y(F_{Q\phi})^{-1} + 2(1-y)(F_{Q\eta})^{-1}} \quad (11)$$

since  $C_H \approx C_Q$  and  $F_{C,Q i,j} = 0$  for  $i \neq j$ . For low loss, the conditions  $F_{C\eta} \gg F_{C\phi}$  and  $F_{Q\eta} \gg F_{Q\phi}$  are satisfied, implying that their contribution to the measurement compatibility is small around  $y = 1$ . As a result, the dominant contribution comes from  $F_{C\phi}$  and  $F_{Q\phi}$ , and the ensuing optimality of the measurement keeps the ratio  $r_H^C$  fairly constant and closer to 1. This behavior can also be seen in Fig. 3, in the low-loss regime with  $y = 0.5$ .

The collective measurements required to attain the HCRB are experimentally challenging to implement. Therefore, with the view of practical feasibility, one must turn towards finite-copy separable measurements, although this comes at a cost of reduced precision. Firstly, we mention that in the case of pure state models, the HCRB is attainable with optimal measurements already at a single-copy level [63]. Secondly, for more general models, a tighter bound known as the Nagaoka-Hayashi Cramér-Rao bound (NHCRB) [43, 64] is attainable with separable measurement on finite number of identical copies of the probe state. It is clear that the use of separable measurements over collective measurements will result in a reduced advantage and the resulting gap between the HCRB and the NHCRB has been studied considering qudits [53].

For the joint-estimation of phase and loss in one arm, a single-copy optimal measurement obtained from the SLD for phase with random single-photon input states of the form:

$|\psi\rangle = c_0|0,1\rangle + c_1|1,0\rangle$  has been demonstrated to fully attain the HCRB for  $\eta_a \geq 0.5$  [58]. Furthermore in [58], it has been numerically demonstrated that there exists certain values of  $N$  and  $\eta_a$  at which this measurement attains the HCRB. This makes our analysis in Section II C 1 much relevant to the practical attainability of the HCRB without the use of collective measurements, in which case the gap between the HCRB and the NHCRB is expected to close. We can conjecture that this is due to the fact that the output probe, in this case, is expressed as a direct

sum of pure states corresponding to the number of lost photons. However, in the cases of phase and loss in both arms (Section II C 2), as well as phase and phase diffusion (Section II D), the loss of direct sum structure may signal the impossibility to attain the HCRB at a single-copy level. Furthermore, it has been shown that if the HCRB cannot be attained at a single-copy level, it can never be attained with any finite number of copies, which makes the single-copy attainability a fundamental one [54]. Of course, collective measurements on infinitely many copies are known to saturate the HCRB, but they are resource inefficient. Nevertheless as mentioned earlier, with finite resources and separable measurements, one can still attain the NHCRB.

#### IV. CONCLUSION

In this work, we have investigated the measurement compatibility in quantum interferometry, considering the joint estimation of phase along with (i) loss in one arm, (ii) loss in both arms, and (iii) phase diffusion in a MZI. These examples are motivated by their practical relevance, but also by conceptual interest: the strong fundamental incompatibility between phase and loss and the weak fundamental compatibility between phase and phase diffusion. We have differentiated the behavior of the measurement compatibility with the fundamental compatibility that is intrinsic to the estimation problem at hand. As our primary aim, we have examined the performance with respect to the HCRB of resource-efficient separable measurements, as opposed to the ideal but experimentally expensive collective measurements. Our results highlight how keeping loss low has the benefit of improving the compatibility of multiparameter estimation, in addition to the usual advantage of increasing the level of practically useful resources.

Multiparameter estimation is by necessity a multifaceted problem, and this entails keeping the attention on all relevant aspects simultaneously. The measurement compatibility  $r_H^C$  does not intend to be an all-encompassing figure, but adds to the quantum estimation toolbox when it comes to considering this one aspect. We thus anticipate it will become commonplace in the analysis of quantum sensing schemes.

#### ACKNOWLEDGMENTS

We thank Francesco Albarelli for stimulating discussion. J. J. and M. S. were supported by the National Science Centre ‘Sonata Bis’ Project No.



2019/34/E/ST2/00273 and the Foundation for Polish Science ‘First Team’ Project No. POIR.04.04.00-00-220E/16-00 (originally, FIRST TEAM/2016-2/17). M. S. was supported by the European Union’s Horizon 2020 research and innovation programme under the Marie Skłodowska-Curie project ‘AppQInfo’ No. 956071, and the QuantERA II Programme that has received funding from the European Union’s Horizon 2020 research and innovation programme under Grant Agreement No. 101017733, project ‘PhoMemtor’ No. 2021/03/Y/ST2/00177. M.B. acknowledges support from the PRIN project PRIN22-RISQUE-2022T25TR3 and MUR Dipartimento di Eccellenza 2023-2027 of the Italian Ministry of University.

## V. APPENDIX

### A. The Holevo Cramér-Rao bound

In Eq. 8, considering a general probe state  $\rho_{\vec{\theta}}$  and setting  $\nu = 1$ , the minimization over  $V$  can be performed analytically which results in the following reformulated version of the HCRB [28].

$$C_H(\rho_{\vec{\theta}}, W, \vec{\theta}) = \min_{\vec{X}} \left[ \text{Tr}(W \text{Re} Z(\vec{X})) + \|\sqrt{W} \text{Im} Z(\vec{X}) \sqrt{W}\|_1 \mid \text{Tr}(\nabla \rho_{\vec{\theta}} \vec{X}^T) = \mathbb{1} \right] \quad (12)$$

where  $\|A\|_1 = \text{Tr}(\sqrt{AA^\dagger})$  is the trace norm. This reformulation is more informative since one can prove that the minimization of only the first term in Eq. 12 gives exactly the QCRB [28] such that

$$\min_{\vec{X}} \text{Tr}(W \text{Re} Z(\vec{X})) = \text{Tr}(W F_Q^{-1}) \quad (13)$$

and when one minimizes Eq. 12 i.e., along with the second term  $\|\sqrt{W} \text{Im} Z(\vec{X}) \sqrt{W}\|_1$ , the contribution due to the fundamental incompatibility is revealed. Thus, it is evident that the imaginary part of  $Z(\vec{X})$  contains information about the fundamental incompatibility.

Furthermore, a necessary and sufficient condition for the equivalence of HCRB and QCRB is given by

$$\text{Tr}(\rho_{\vec{\theta}}[L_{\theta_i}, L_{\theta_j}]) = 0, \quad \forall \theta_i, \theta_j \in \Theta, i \neq j \quad (14)$$

This condition is known as the commutation condition [21, 63, 65, 66] indicating weak compatibility.

### B. Measurement compatibility with respect to the weights under varying loss on the reference arm

In this section, we demonstrate the behavior of measurement compatibility with respect to the weights for the double homodyne measurement as one varies the loss on the reference arm  $\eta_b$  by keeping  $\eta_a$  at a fixed value. In Fig. 5, we have obtained the plots for gHB states with  $N = 2, 3, 4$  and HB states with  $N = 2, 4$ . In the regime of high losses on the reference arm i.e.,  $\eta_b = 0.1$ , the overall value of  $r_H^C$  decreases as  $N$  increases. However, with  $\eta_b = 0.5$ , there is a crossing at  $y = 0.6$ . When the loss in the reference arm is low, the overall value of  $r_H^C$  increases as  $N$  increases. We infer that these features are an artifact of the measurement since they remain qualitatively the same for the class of probe states considered here.

### C. Compatibility with respect to the weights under minimal losses

In this section, in Fig. 6, we depict the behavior of both measurement and fundamental compatibilities with respect to the weights under minimal losses in both arms i.e.,  $\eta_a = \eta_b = 0.999$  for gHB and HB states with  $N = 2, 4, 6$ . Considering  $r_H^C$  for  $y = 1$  (phase estimation), due to the manifestation of the optimality of the double homodyne measurement, we get  $r_H^C = 1$ . However, the value of  $r_H^C$  remains below 1.5 until  $y = 0.5$  which indicates that, in the multi-parameter setting, even though the optimality for a joint estimation is non-achievable, the measurement compatibility performs very well. On the other hand, we find that the value of  $r_{BG} \approx 1$  for all values of  $y$ .

Therefore, since the double homodyne measurement is optimal for phase estimation, one finds higher compatibility when weights are chosen closer to phase estimation. As weights are chosen closer to loss estimation, the sub-optimality or the incompatibility of the measurement in estimating loss becomes more pronounced leading to higher values of  $r_H^C$  (refer to Eq. 11). At the same time, as we are estimating extremely low values of losses, the joint-estimation of phase and loss effectively becomes a single-parameter phase estimation problem for which  $C_H \approx C_Q$ . However, the incompatibility term in  $C_H$  becomes more pronounced when one estimates higher values of losses. Thus, in the case of very low losses, the interplay of  $C_C$ ,  $C_H$ , and  $C_Q$ , combined with the parameter weights, gives rise to a region where the HCRB is closely attainable with the double homodyne measurement on individual copies of the probe.

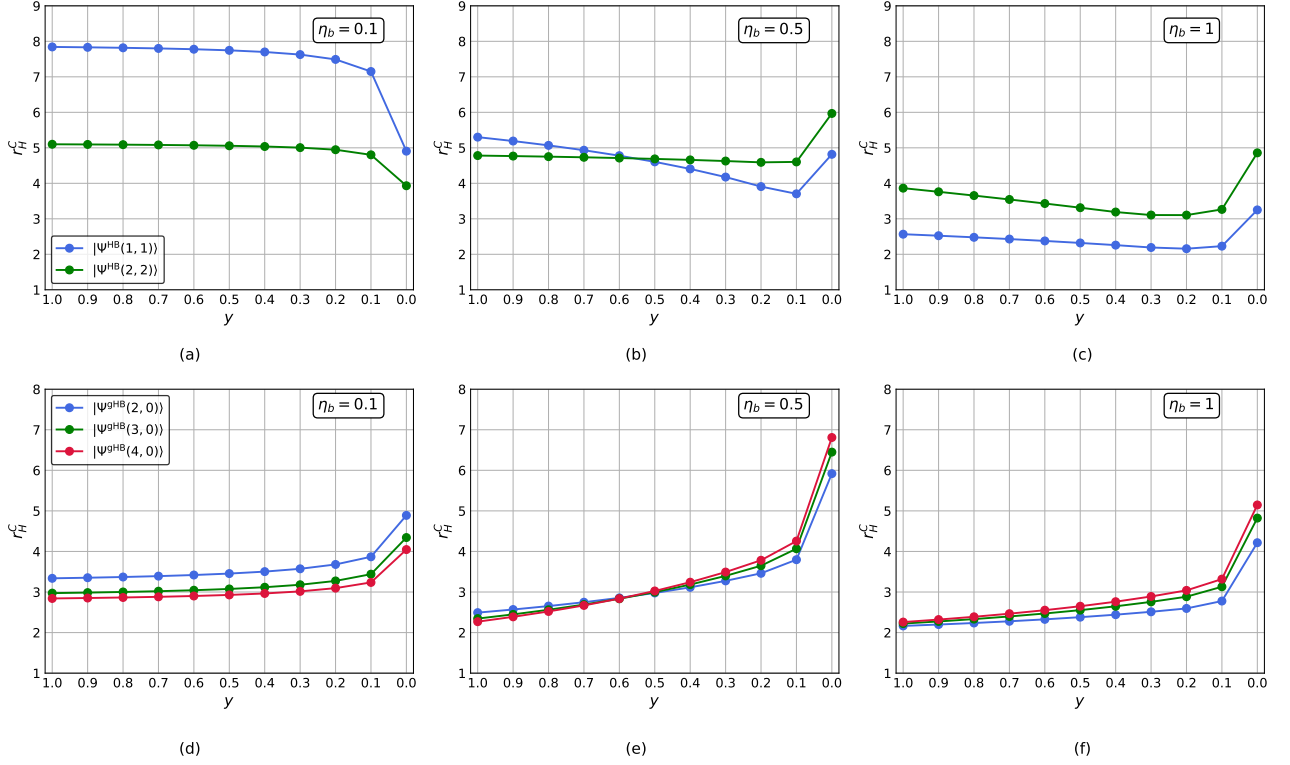


FIG. 5. *Top row:* Plot of measurement compatibility measure  $r_H^C$  versus the weights  $y$  for the joint-estimation of phase and loss considering HB states with  $N = 2, 4$  at different values of loss on reference arm, namely,  $\eta_b = 0.1$ ,  $\eta_b = 0.5$ , and  $\eta_b = 1$ . *Bottom row:* The same plots for gHB states with  $N = 2, 3, 4$ . The double homodyne measurement is considered and the curves in all the panels are plotted at  $\eta_a = 0.5$  and  $\Delta = 0$ .

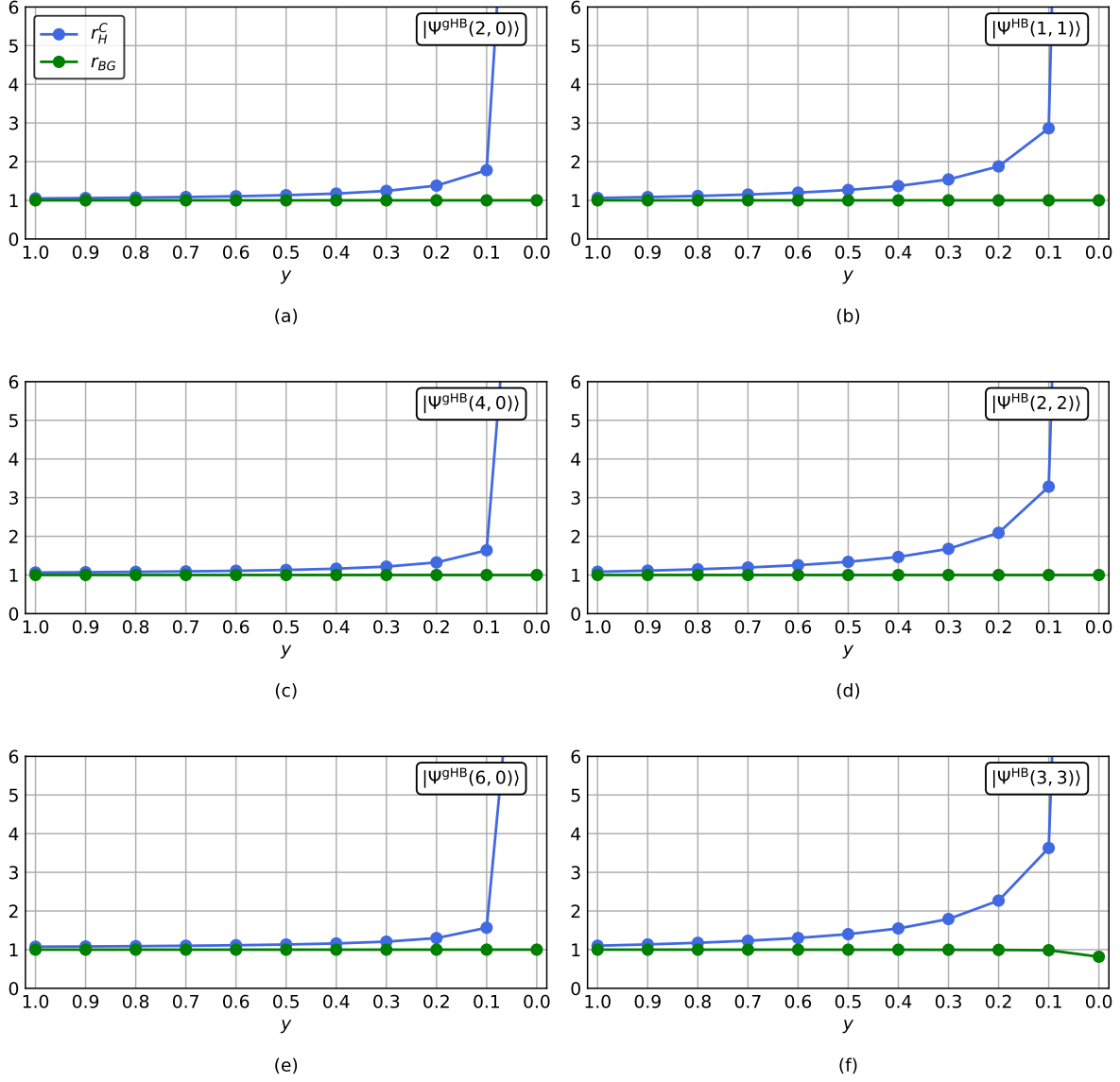


FIG. 6. Plot of measurement compatibility  $r_H^C$  and fundamental compatibility  $r_{BG}$  versus the weights  $y$  for the joint-estimation of phase and loss with  $\eta_a = \eta_b = 0.999$  and  $\Delta = 0$  (minimal losses). gHB and HB states with  $N = 2, 4, 6$  and double homodyne measurement are considered here. Note that for  $y \geq 0.5$ ,  $r_H^C$  remains below 1.5 implying that the HCRB is closely attained by the double homodyne measurement.

- 
- [1] V. Giovannetti, S. Lloyd, and L. Maccone, *Science* **306**, 1330 (2004).
  - [2] M. G. Paris, *International Journal of Quantum Information* **7**, 125 (2009).
  - [3] R. Demkowicz-Dobrzański, M. Jarzyna, and J. Kołodyński, *Progress in Optics* **60**, 345 (2015).
  - [4] N. P. Mauranyapin, A. Terrasson, and W. P. Bowen, *Advanced Quantum Technologies* **5**, 2100139 (2022).
  - [5] C. M. Caves, *Physical Review D* **23**, 1693 (1981).
  - [6] J. J. Bollinger, W. M. Itano, D. J. Wineland, and D. J. Heinzen, *Physical Review A* **54**, R4649 (1996).
  - [7] D. Branford, C. N. Gagatsos, J. Grover, A. J. Hickey, and A. Datta, *Physical Review A* **100**, 022129 (2019).
  - [8] G. Atkinson, E. Allen, G. Ferranti, A. McMillan, and J. Matthews, *Physical Review Applied* **16**, 044031 (2021).
  - [9] L. Pezzé and A. Smerzi, *Physical review letters* **100**, 073601 (2008).
  - [10] K. P. Seshadreesan, P. M. Anisimov, H. Lee, and J. P. Dowling, *New Journal of Physics* **13**, 083026 (2011).
  - [11] G. d'Ariano, C. Macchiavello, and M. G. Paris, *Physics Letters A* **198**, 286 (1995).
  - [12] K. Banaszek, R. Demkowicz-Dobrzański, and I. A. Walmsley, *Nature Photonics* **3**, 673 (2009).
  - [13] L. Maccone and V. Giovannetti, *Nature Physics* **7**, 376 (2011).
  - [14] U. Dorner, R. Demkowicz-Dobrzanski, B. J. Smith, J. S. Lundeen, W. Wasilewski, K. Banaszek, and I. A. Walmsley, *Physical review letters* **102**, 040403 (2009).
  - [15] R. Demkowicz-Dobrzanski, U. Dorner, B. Smith, J. Lundeen, W. Wasilewski, K. Banaszek, and I. Walmsley, *Physical Review A—Atomic, Molecular, and Optical Physics* **80**, 013825 (2009).
  - [16] H. Cable and G. A. Durkin, *Physical review letters* **105**, 013603 (2010).
  - [17] S. Knysh, V. N. Smelyanskiy, and G. A. Durkin, *Physical Review A—Atomic, Molecular, and Optical Physics* **83**, 021804 (2011).
  - [18] B. Escher, R. L. de Matos Filho, and L. Davidovich, *Nature Physics* **7**, 406 (2011).
  - [19] J. Kolodyński, *arXiv preprint arXiv:1409.0535* (2014).
  - [20] R. Nichols, P. Liuzzo-Scorpo, P. A. Knott, and G. Adesso, *Physical Review A* **98**, 012114 (2018).
  - [21] P. J. Crowley, A. Datta, M. Barbieri, and I. A. Walmsley, *Physical Review A* **89**, 023845 (2014).
  - [22] M. Altorio, M. G. Genoni, M. D. Vidrighin, F. Somma, and M. Barbieri, *Physical Review A* **92**, 032114 (2015).
  - [23] M. D. Vidrighin, G. Donati, M. G. Genoni, X.-M. Jin, W. S. Kolthammer, M. Kim, A. Datta, M. Barbieri, and I. A. Walmsley, *Nature communications* **5**, 3532 (2014).
  - [24] M. Szczykulska, T. Baumgratz, and A. Datta, *Quantum Science and Technology* **2**, 044004 (2017).
  - [25] J. Jayakumar, M. E. Mycroft, M. Barbieri, and M. Stobińska, *New Journal of Physics* **26**, 073016 (2024).
  - [26] X.-M. Lu and X. Wang, *Physical Review Letters* **126**, 120503 (2021).
  - [27] I. Kull, P. A. Guérin, and F. Verstraete, *Journal of Physics A: Mathematical and Theoretical* **53**, 244001 (2020).
  - [28] S. Ragy, M. Jarzyna, and R. Demkowicz-Dobrzański, *Physical Review A* **94**, 052108 (2016).
  - [29] C. W. Helstrom, *Journal of Statistical Physics* **1**, 231 (1969).
  - [30] S. L. Braunstein and C. M. Caves, *Physical Review Letters* **72**, 3439 (1994).
  - [31] J. Liu, H. Yuan, X.-M. Lu, and X. Wang, *Journal of Physics A: Mathematical and Theoretical* **53**, 023001 (2020).
  - [32] A. S. Holevo, *Probabilistic and statistical aspects of quantum theory*, Vol. 1 (Springer Science & Business Media, 2011).
  - [33] M. Hayashi and K. Matsumoto, *Journal of Mathematical Physics* **49** (2008).
  - [34] E. Roccia, I. Gianani, L. Mancino, M. Sbroscia, F. Somma, M. G. Genoni, and M. Barbieri, *Quantum Science and Technology* **3**, 01LT01 (2017).
  - [35] M. Parniak, S. Borówka, K. Boroszko, W. Wasilewski, K. Banaszek, and R. Demkowicz-Dobrzański, *Physical review letters* **121**, 250503 (2018).
  - [36] L. O. Conlon, T. Vogl, C. D. Marciniak, I. Pogorelov, S. K. Yung, F. Eilenberger, D. W. Berry, F. S. Santana, R. Blatt, T. Monz, *et al.*, *Nature Physics* **19**, 351 (2023).
  - [37] Z. Hou, J.-F. Tang, J. Shang, H. Zhu, J. Li, Y. Yuan, K.-D. Wu, G.-Y. Xiang, C.-F. Li, and G.-C. Guo, *Nature communications* **9**, 1414 (2018).
  - [38] Y. Yuan, Z. Hou, J.-F. Tang, A. Streltsov, G.-Y. Xiang, C.-F. Li, and G.-C. Guo, *npj Quantum Information* **6**, 46 (2020).
  - [39] L. O. Conlon, F. Eilenberger, P. K. Lam, and S. M. Assad, *Communications Physics* **6**, 337 (2023).
  - [40] C. W. Helstrom, *Physics letters A* **25**, 101 (1967).
  - [41] C. Helstrom, *IEEE Transactions on information theory* **14**, 234 (1968).
  - [42] H. Yuen and M. Lax, *IEEE Transactions on Information Theory* **19**, 740 (1973).
  - [43] M. Hayashi, *Asymptotic theory of quantum statistical inference: selected papers* (World Scientific, 2005).
  - [44] A. Carollo, B. Spagnolo, A. A. Dubkov, and D. Valenti, *Journal of Statistical Mechanics: Theory and Experiment* **2019**, 094010 (2019).
  - [45] M. Tsang, F. Albarelli, and A. Datta, *Physical Review X* **10**, 031023 (2020).
  - [46] R. Demkowicz-Dobrzański, W. Górecki, and M. Guță, *Journal of Physics A: Mathematical and Theoretical* **53**, 363001 (2020).
  - [47] F. Bellardo and V. Giovannetti, *New Journal of Physics* **23**, 063055 (2021).
  - [48] M. Guță and J. Kahn, *Physical Review A—Atomic,*

- Molecular, and Optical Physics **73**, 052108 (2006).
- [49] J. Kahn and M. Guță, *Communications in Mathematical Physics* **289**, 597 (2009).
  - [50] S. Massar and S. Popescu, *Physical review letters* **74**, 1259 (1995).
  - [51] K. Yamagata, A. Fujiwara, and R. D. Gill, *Annals of Statistics* **41**, 2197 (2013).
  - [52] Y. Yang, G. Chiribella, and M. Hayashi, *Communications in Mathematical Physics* **368**, 223 (2019).
  - [53] A. Das, L. O. Conlon, J. Suzuki, S. K. Yung, P. K. Lam, and S. M. Assad, *arXiv preprint arXiv:2405.09622* (2024).
  - [54] L. Conlon, J. Suzuki, P. Lam, and S. Assad, *arXiv preprint arXiv:2208.07386* (2022).
  - [55] E. Roccia, V. Cimini, M. Sbroscia, I. Gianani, L. Ruggiero, L. Mancino, M. G. Genoni, M. A. Ricci, and M. Barbieri, *Optica* **5**, 1171 (2018).
  - [56] F. Belliardo, V. Cimini, E. Polino, F. Hoch, B. Piccirillo, N. Spagnolo, V. Giovannetti, and F. Sciarrino, *Phys. Rev. Res.* **6**, 023201 (2024).
  - [57] M. E. Mycroft, T. McDermott, A. Buraczewski, and M. Stobińska, *Physical Review A* **107**, 012607 (2023).
  - [58] F. Albarelli, J. F. Friel, and A. Datta, *Physical review letters* **123**, 200503 (2019).
  - [59] M. Zhang, H.-M. Yu, H. Yuan, X. Wang, R. Demkowicz-Dobrzański, and J. Liu, *Physical Review Research* **4**, 043057 (2022).
  - [60] M. ApS, *MOSEK Fusion API for Python 10.2.12* (2019).
  - [61] J. Jayakumar, *HCRB for gHB states* (2025).
  - [62] A. Fujiwara, *Physical Review A* **63**, 042304 (2001).
  - [63] K. Matsumoto, *Journal of Physics A: Mathematical and General* **35**, 3111 (2002).
  - [64] L. O. Conlon, J. Suzuki, P. K. Lam, and S. M. Assad, *npj Quantum Information* **7**, 110 (2021).
  - [65] C. Vaneph, T. Tufarelli, and M. G. Genoni, *Quantum Measurements and Quantum Metrology* **1**, 12 (2013).
  - [66] J. Suzuki, *Journal of Mathematical Physics* **57** (2016).